JOURNAL OF THE ROYAL SOCIETY Interface

rsif.royalsocietypublishing.org

Research

Cite this article: Brodersen KE, Lichtenberg M, Ralph PJ, Kühl M, Wangpraseurt D. 2014 Radiative energy budget reveals high photosynthetic efficiency in symbiont-bearing corals. *J. R. Soc. Interface* **11**: 20130997.
http://dx.doi.org/10.1098/rsif.2013.0997

Received: 30 October 2013
Accepted: 8 January 2014

Subject Areas:
bioenergetics, biochemistry

Keywords:
light energy budget, microsensors, light utilization, thermal boundary layer, photosynthetic efficiency, bio-optics

Author for correspondence:
Michael Kühl
e-mail: mkuhl@bio.ku.dk

†These authors contributed equally to this study.

Electronic supplementary material is available at http://dx.doi.org/10.1098/rsif.2013.0997 or via http://rsif.royalsocietypublishing.org.

Royal Society Publishing

Radiative energy budget reveals high photosynthetic efficiency in symbiont-bearing corals

Kasper Elgetti Brodersen[1,2,†], Mads Lichtenberg[1,†], Peter J. Ralph[2], Michael Kühl[1,2,3] and Daniel Wangpraseurt[2]

[1]Marine Biological Section, Department of Biology, University of Copenhagen, Strandpromenaden 5, Helsingør 3000, Denmark
[2]Plant Functional Biology and Climate Change Cluster, University of Technology, Sydney, 15 Broadway, Ultimo, Sydney, NSW 2007, Australia
[3]Singapore Centre on Environmental Life Sciences Engineering, School of Biological Sciences, Nanyang Technological University, Singapore, Republic of Singapore

The light field on coral reefs varies in intensity and spectral composition, and is the key regulating factor for phototrophic reef organisms, for example scleractinian corals harbouring microalgal symbionts. However, the actual efficiency of light utilization in corals and the mechanisms affecting the radiative energy budget of corals are underexplored. We present the first balanced light energy budget for a symbiont-bearing coral based on a fine-scale study of the microenvironmental photobiology of the massive coral *Montastrea curta*. The majority (more than 96%) of the absorbed light energy was dissipated as heat, whereas the proportion of the absorbed light energy used in photosynthesis was approximately 4.0% under an irradiance of 640 µmol photons m^{-2} s^{-1}. With increasing irradiance, the proportion of heat dissipation increased at the expense of photosynthesis. Despite such low energy efficiency, we found a high photosynthetic efficiency of the microalgal symbionts showing high gross photosynthesis rates and quantum efficiencies (QEs) of approximately 0.1 O_2 $photon^{-1}$ approaching theoretical limits under moderate irradiance levels. Corals thus appear as highly efficient light collectors with optical properties enabling light distribution over the corallite/tissue microstructural canopy that enables a high photosynthetic QE of their photosynthetic microalgae *in hospite*.

1. Introduction

Coral reefs are among the most productive and diverse ecosystems on the Earth despite being situated mainly in oligotrophic tropical waters. The evolutionary success of this important ecosystem is largely attributed to the successful symbiosis between the coral host (a cnidarian) and its photosynthetic microalgal endosymbionts (dinoflagellates in the genus *Symbiodinium*). These so-called zooxanthellae excrete photosynthates, which can provide up to 95% of the energy demand of their cnidarian hosts [1,2]. Photosynthesis is the process where solar energy is converted into chemical energy and stored as biomass in phototrophic organisms. It is driven by photons absorbed by pigment–protein complexes resulting in a charge separation at the two reaction centres of the photosystems [3,4]. At low irradiance, the photosynthesis is limited by the rate of energy supply to the photosystems, whereas at higher irradiances enzymatic reactions limit the rate of energy transformation and thus lead to the increasing saturation of photosynthesis with irradiance [3]. Excess absorbed light energy that is not used for photosynthesis, especially at high photon fluxes, is dissipated as heat and fluorescence. Dissipation of excess light energy as heat is in part because of various photoregulatory mechanisms termed non-photochemical quenching (NPQ). NPQ is used by photosynthetic cells under high light to avoid photodamage, such as degradation of pigments and enzymes by reactive oxygen species produced in de-excitation of the triplet state of Chl ($^3Chl^*$) [3,5].

Photosynthetic organisms employ various mechanisms to avoid photodamage, where heat dissipation through NPQ is just one effective short-term way to get rid of excess energy. Long-term regulation, and thereby protection, can be achieved by regulating the amount of light-harvesting and carotenoid pigments [6,7]. Corals acclimatized to high irradiance often appear more transparent than those acclimatized to low light conditions owing to lower pigment concentrations per cell or the spatial organization of chloroplasts ensuring a lower absorption cross section [8]. Another long-term regulatory mechanism in corals is to upregulate the expression of protective coral host pigments, which absorb light in the blue to orange region of the photosynthetically active radiation (PAR) spectrum without inducing oxygenic photosynthesis [9–10]. Host pigment absorption and subsequent energy dissipation via reflection or fluorescence of photons may thus result in lower photosynthetic quantum efficiencies (QEs) but host pigments may also ensure photoprotection in high irradiance environments [11,12] and might give rise to scattering phenomena and wavelength transformations that could enhance photosynthesis [11,13]. However, some other members of the large family of GFP-like host pigments fulfil presumably different as yet unresolved functions in reef corals [14].

Absorbed solar radiation can also drive an increase in the surface temperature of corals relative to the ambient seawater [15–17] and such warming correlates linearly with incident irradiance [15]. The increase in surface temperature is counterbalanced by convective heat transfer to the surrounding water, leading to the establishment of a thermal boundary layer (TBL) [15]. The presence of a TBL limits the rate of convective heat dissipation from the coral surface, as the TBL acts as an insulating barrier, the thickness of which is decreasing with the inverse power of the flow velocity [18]. The TBL behaves analogous to the diffusive boundary layer, which at low flow velocity impedes mass transfer and thereby affects coral gas exchange and nutrient uptake [19–21] as well as the rate of photosynthesis and respiration [15,22,23].

Corals in shallow reef habitats are exposed to high downwelling irradiance of more than 2000 µmol photons m^{-2} s^{-1}, especially during midday low-tide periods [16]. The variability of light in the reef environment is not only underlying diurnal dynamics modulated by tides but corals also experience pulses of high intensity light exposure owing to wave focusing producing short duration flashes of more than 9000 µmol photons m^{-2} s^{-1}, with up to more than 350 light flashes per minute in shallow waters [24]. Excess absorbed light energy can lead to photoinhibition and damage the photosystems and coral light absorption can increase the temperature in the coral microenvironment, potentially aggravating negative responses to elevated seawater temperatures [15,18]. High irradiance in combination with elevated water and coral tissue temperatures can induce a cascade of stress responses in corals ultimately leading to the breakdown of the algal–cnidarian symbiosis (owing to the excretion of symbionts and/or pigment degradation of the algal symbiont), which is termed as coral bleaching [25–28]. Moreover, nutrient starvation reduces the photosynthetic efficiency of zooxanthellae and renders corals more susceptible to bleaching [29]. This demonstrates the importance of understanding the mechanisms regulating radiative energy dissipation and the fate of absorbed light energy within corals.

It has been shown that corals are highly efficient at collecting [30,31] and using solar radiation [32,33]. It is known that more than 90% of incident PAR (400–700 nm) can be absorbed by corals and calculations have suggested that their QEs are close to theoretical limits (i.e. 0.125 O_2 photon^{-1} as eight photons are needed to separate the electrons required to produce one O_2 molecule [3,32,34]). There is also mounting evidence that corals have unique optical properties that could relate such high efficiency to efficient light capture [21,30,35,36]. However, a closed radiative energy budget for corals and direct microscale measurements of the photosynthetic QE of zooxanthellae *in hospite* are lacking.

In this study, we apply an experimental approach developed for photosynthetic biofilms [37] to determine the first balanced light energy budget of a coral as a function of incident irradiance and flow velocity. This was obtained by combining fibre-optic and electrochemical microsensor measurements of light reflectance and absorption, rates of gross photosynthesis (GPP) and coral tissue surface warming. Such detailed measurements of the main energy dissipating mechanisms in coral tissue allowed us to estimate the proportion of the absorbed light energy used by photosynthesis and dissipated as heat, respectively. Furthermore, such measurements provided the first measurements of the local QE of zooxanthellae photosynthesis at depth within coral tissue.

2. Material and methods

2.1. Coral samples

Coral specimens were collected from shallow waters (less than 3 m depths) on the reef flat of the Heron Island lagoon, Great Barrier Reef, Australia (152°06′ E, 20°29′ S). The coral *Montastrea curta* was chosen as highly suitable for intratissue microsensor measurements owing to its thick tissue and minimal mucus secretion. Specimens were transported to the coral holding facility at the University of Technology, Sydney, where corals were acclimated and maintained under continuous flow at 25°C, salinity of 33 and moderate levels of downwelling irradiance (150–200 µmol photons m^{-2} s^{-1}; 400–700 nm; 12 D : 12 L cycle).

2.2. Experimental set-up

Small fragments of *M. curta* were placed in a custom-made black acrylic flow-through chamber for at least 45 min prior to the microsensor measurements to ensure steady-state O_2 and temperature conditions (as confirmed from repeated microprofile measurements). Corals were illuminated with a defined irradiance regime and were continuously flushed with aerated seawater (25°C and a salinity of 33) at an average flow velocity of either approximately 0.4 or 0.8 cm s^{-1} as maintained by a submerged water pump in a 20 l thermostated aquarium reservoir.

Illumination was provided by a fibre-optic tungsten halogen lamp (KL-2500, Schott GmbH, Germany) equipped with an internal heat filter and a collimating lens positioned vertically above the flow-through chamber (figure 1). The light intensity of the lamp could be regulated without spectral distortion by a built-in filter wheel with pinholes of various sizes. The downwelling quantum irradiance in the PAR range (400–700 nm) (E_d in µmol photons m^{-2} s^{-1}) was measured with a calibrated quantum irradiance meter (ULM-500, Walz GmbH, Germany) equipped with a planar cosine collector (LI-192S, LiCor, USA). The experimental irradiances (160, 320, 640, 1280 and 2400 µmol photons m^{-2} s^{-1}) were achieved by adjusting the aperture on the fibre-optic halogen lamp without any spectral distortion. The downwelling spectral irradiance at the above-mentioned quantum irradiance levels was also measured in radiometric energy units (in W m^{-2} nm^{-1}) with a calibrated spectroradiometer (Jaz A0523, Ocean Optics, Dunedin, FL,

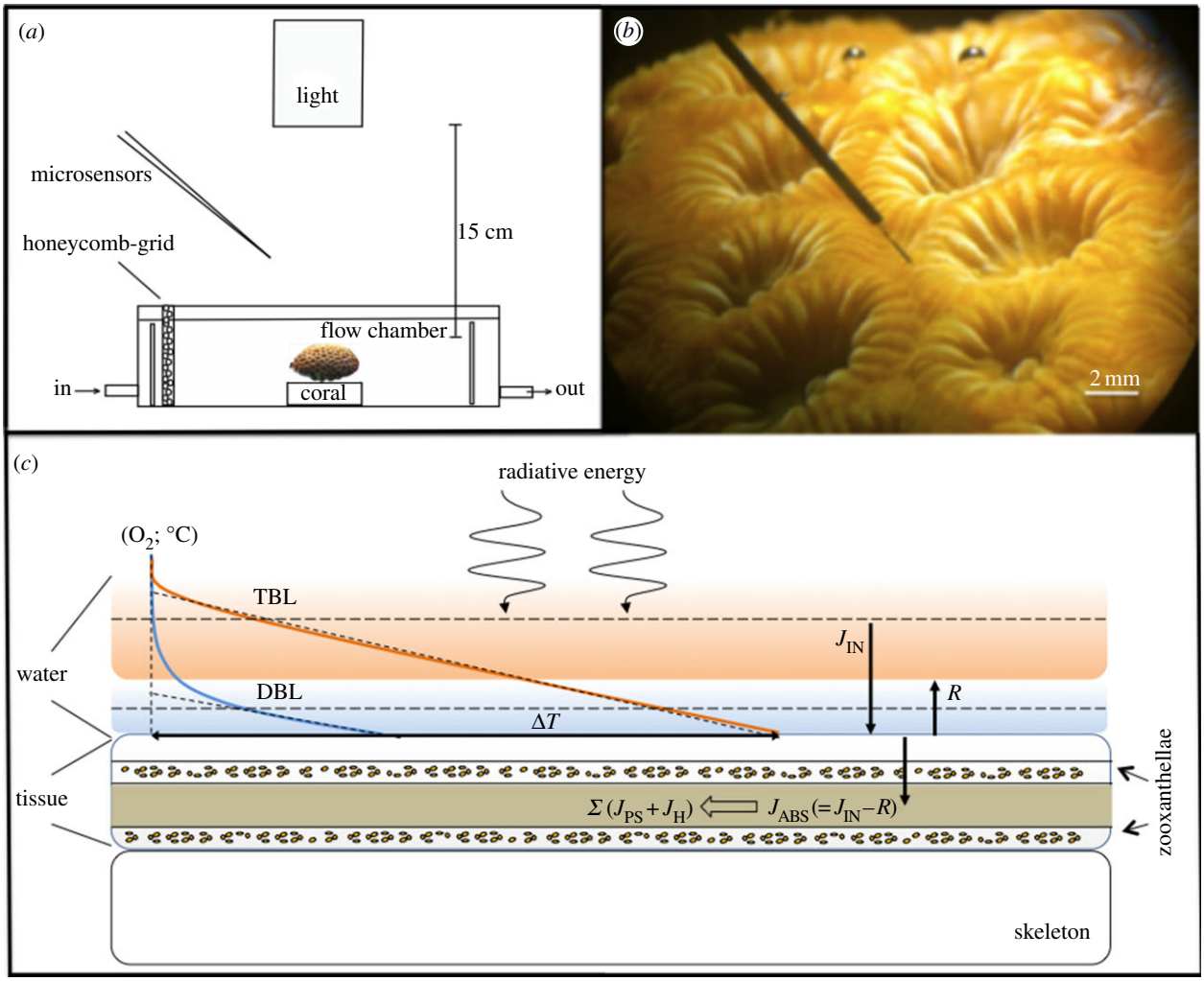

Figure 1. Experimental setup. (*a*) Schematic of the experimental setup visualizing the relative position of light source, microsensors and coral fragment. (*b*) A scalar irradiance microsensor inserted into the coenosarc tissue of a *M. curta* coral. (*c*) Conceptual diagram showing the fate of light energy (abbreviations explained in text).

USA). The coral fragment was positioned at the centre of the light beam. The complete set-up was covered with a black cloth to avoid stray light.

2.3. Microsensor measurements

Spectral scalar irradiance, $E_0(\lambda)$, was measured with a fibre-optic scalar irradiance microprobe (integrating sphere diameter approx. 100 µm [38,39]) connected to a fibre-optic spectrometer (USB 2000+, Ocean Optics, USA). We used a black non-reflective light well to measure the incident downwelling spectral irradiance, $E_d(\lambda)$ table 1, at the same distance from the light source as done with the measurements on the coral surface; in a collimated light beam the downwelling scalar irradiance and the downwelling irradiance are identical [40]. The spectral reflectance was measured with a fibre-optic field radiance microprobe [41,42].

Oxygen concentrations were measured with Clark-type microelectrodes (tip diameter approx. 25 µm, OX-25, Unisense A/S, Aarhus, Denmark) with a fast response time (less than 0.5 s) and a low stirring sensitivity (less than 1–2%) [43,44]. The microsensor was connected to a pA-meter (Unisense A/S) and was linearly calibrated, at experimental temperature and salinity, from measurements in aerated (free-flowing part of the flow chamber) and anoxic seawater (flushed with N_2).

Temperature measurements were performed with a thermocouple microsensor (tip diameter approx. 50 µm; T50, Unisense A/S) connected to a thermocouple meter (Unisense A/S). The temperature microsensors were linearly calibrated against a high precision thermometer (Testo 110, Testo AG, Germany; accuracy ±0.2°C) in seawater at different temperatures. Both temperature and O_2 microsensors were connected to an A/D converter (DCR-16, Pyroscience GmbH, Germany) interfaced with a PC running data acquisition software (ProFix, Pyroscience GmbH).

Microsensor measurements of spectral scalar irradiance, spectral radiance, O_2 and temperature were done with the sensors approaching the coral surface at a 45° angle relative to the vertically incident light beam to avoid self-shading. The microsensors were mounted on a PC-interfaced motorized micromanipulator (MU-1, PyroScience, GmbH) controlled by dedicated data acquisition and positioning software (ProFix, Pyros-Science GmbH); the software automatically corrected for the sensor inclination and all depths are given in vertical distances.

The microsensor was positioned at the coral tissue surface (defined as 0 µm depth) by means of the micromanipulator and observed using a stereo-microscope (7×–90×, AmScope, Irvine, CA, USA). Microsensor measurements of temperature, O_2 and scalar irradiance on and within coral coenosarc tissue were performed as described previously [15,35] (see figure 1). All profiles were measured in vertical steps of 100 µm. Within the tissue, microprofiles were performed from the tissue surface until the skeleton was reached, which could be observed by a slight bending of the microsensors and enhanced noise in the O_2 signal.

2.4. Irradiance calculations

The spectral scalar irradiance, $E_0(\lambda)$, was measured in vertical depth steps throughout the coral tissue and calculated as the fraction of the incident downwelling irradiance, $E_0(\lambda)/E_d(\lambda)$. By multiplying the normalized scalar irradiance spectra with the measured spectra of absolute downwelling irradiance at the

Table 1. Terms, definitions and units. PAR denotes photosynthetically active radiation (400–700 nm).

$E_d(\lambda)$	downwelling spectral scalar irradiance	(μmol photons m^{-2} s^{-1} nm^{-1})
$E_0(\lambda)$	spectral scalar irradiance at depth, z	(μmol photons m^{-2} s^{-1} nm^{-1})
$E_E(\lambda)$	absolute downwelling irradiance	(W m^{-2} nm^{-1})
E_0(PAR)	photon scalar irradiance (PAR)	(μmol photons m^{-2} s^{-1})
J_{ABS}	absorbed light energy, vector irradiance (PAR)	(J m^{-2} s^{-1})
$E_{ABS}(z)$	local density of absorbed light	(μmol photons m^{-3} s^{-1})
R(PAR)	PAR irradiance reflectance	(W m^{-2} nm^{-1})
K_0(PAR)	diffuse attenuation coefficient (PAR)	(mm^{-1})
A(PAR)	absorption coefficient (PAR)	(mm^{-1})
$K_0(\lambda)$	spectral attenuation coefficient	(mm^{-1})
J_{GPP}	areal rates of GPP	(nmol O_2 cm^{-2} s^{-1})
J_{PS}	areal rates of GPP, in energy units	(J m^{-2} s^{-1})
P_{max}	photochemical energy conservation	(J m^{-2} s^{-1})
PS(z)	volumetric rate of GPP at depth z	(nmol O_2 cm^{-3} s^{-1})
PS_{max}	local photosynthesis maximum	(nmol O_2 cm^{-3} s^{-1})
J_H	energy dissipation as heat	(J m^{-2} s^{-1})
$\eta(z)$	local photosynthetic quantum efficiency	(O_2 $photon^{-1}$)

coral tissue surface (in W m^{-2} nm^{-1}) as measured by a calibrated spectrometer (Jaz, Ocean optics, USA), we obtained the absolute energy levels of scalar irradiance at the different measuring depths. We converted the absolute scalar irradiance spectra to photon scalar irradiance spectra (in µmol photons m^{-2} s^{-1} nm^{-1}) by using Planck's equation:

$$E_\lambda = h \cdot \frac{c}{\lambda},$$

where E_λ is the energy of a photon, λ the wavelength, h Planck's constant (6.626×10^{-34} W s^2) and c the speed of light in vacuum (in m s^{-1}). The light attenuation in the tissue was calculated by integrating the spectral photon irradiance over PAR (420–700 nm) yielding a measure of PAR photon scalar irradiance (in µmol photons m^{-2} s^{-1}), i.e. light energy available for oxygenic photosynthesis at a given tissue depth. Light less than 420 nm was strongly absorbed in the upper tissue and light measurements in this wavelength range exhibited increasing amounts of stray light from within the spectrometer and were therefore not included.

The PAR irradiance reflectance of the coral tissue surface was calculated as

$$R(\mathrm{PAR}) = \int_{420}^{700} \frac{E_u(\lambda)}{E_d(\lambda)} d\lambda,$$

where $E_u(\lambda)$ is the upwelling irradiance at the coral tissue surface, here estimated as the backscattered spectral radiance measured at the coral tissue surface [42], and $E_d(\lambda)$ is the downwelling irradiance estimated as the backscattered spectral radiance measured over a white reflectance standard (Spectralon; Labsphere, North Sutton, NH, USA). R(PAR) measurements rely on the assumption that the backscattered light from the tissue surface was entirely diffused [30,35,40].

The absorbed light energy (J_{ABS}; in J m^{-2} s^{-1}) within the coral tissue and thus available for photosynthesis was calculated by subtracting the downwelling and upwelling irradiance at the tissue surface, as calculated by

$$J_{ABS}(\mathrm{PAR}) = \int_{420}^{700} E_d(\lambda)(1 - R(\lambda))\, d\lambda,$$

where $E_d(\lambda)$ and $R(\lambda)$ are the downwelling spectral irradiance and irradiance reflectance, respectively. The parameter J_{ABS} is equivalent to the so-called vector irradiance, which is a measure of the net downwelling energy flux [40].

2.5. Temperature and O_2 calculations

GPP was measured with O_2 microsensors using the light–dark shift method, which allows photosynthesis estimates independent of light respiration [45]. Areal rates of GPP (J_{GPP}; in nmol O_2 cm^{-2} s^{-1}) were calculated by depth integration of the volumetric rates (in nmol O_2 cm^{-3} s^{-1}) measured in different depths over the euphotic zone, i.e. throughout the photosynthetic coral tissue.

The total amount of energy used by photosynthesis in the coral tissue (J_{PS}; in J m^{-2} s^{-1}) was calculated by multiplying the areal GPP rate with the Gibbs free energy (482.9 kJ $(mol\ O_2)^{-1}$), i.e. the energy released through O_2 and adenosine triphosphate formation [37,46]:

$$J_{PS} = J_{GPP} E_G.$$

Light energy that was not used in photosynthesis resulted in a local increase of the coral tissue surface temperature leading to the establishment of a TBL [15]. The heat dissipation ($J_{H,up}$; in J m^{-2} s^{-1}), i.e. the heat flux from the coral tissue into the water column, was estimated from the temperature flux across the TBL and was calculated by Fourier's law of conduction:

$$J_{H,up} = k \frac{\partial T}{\partial z},$$

where k is the thermal conductivity in seawater (0.6 W m^{-1} K^{-1} [47]) and $\partial T/\partial z$ is the measured linear temperature gradient in the TBL.

As microsensor measurements of heat conduction into coral skeleton are very challenging because of high risk of sensor breakage, the downward flux of heat into the coral skeleton was calculated as $J_{H,down} = J_{ABS} - (J_{H,up} + J_{PS})$. The total amount of energy dissipated as heat in the coral tissue (J_H; in J m^{-2} s^{-1}) was then calculated as $J_H = J_{H,up} + J_{H,down}$.

2.6 Light energy budget and photosynthetic efficiency calculations

To estimate the overall radiative energy utilization efficiency of the system, the balanced light energy budget was determined

by the following equations:

$$J_{IN} = J_H + J_{PS} + R \quad \text{and} \quad J_{IN} - R = J_{ABS} = J_{PS} + J_H,$$

where J_{IN} is the total incoming light energy flux; J_H is the amount of the incoming light energy dissipated as heat; J_{PS} is the amount of the incoming light energy used by photosynthesis; R is the amount of incident light energy backscattered from the coral tissue surface and thus lost from the system; and J_{ABS} is the amount of the incoming light energy absorbed by the system. The final balanced light energy budget characterized the tissue as a homogeneous layer, ignoring any vertical microheterogeneity in symbiont distribution and was defined as

$$J_{ABS} = J_{PS} + J_H$$

assuming a 1 : 1 stoichiometry of CO_2 fixation and O_2 production, i.e. the energy stored in the light-dependent reaction is completely used for CO_2 fixation in the dark reaction, and that autofluorescence from the tissue is negligible [37].

ε_{PS} and ε_H represent the efficiencies of photosynthetic energy conservation and heat dissipation at a given absorbed light energy (J_{ABS}), respectively, and were calculated as [37]

$$\varepsilon_{PS} = \frac{J_{PS}(J_{abs})}{J_{abs}} \quad \text{and} \quad \varepsilon_H = \frac{J_H(J_{abs})}{J_{abs}}.$$

The photon scalar irradiance of PAR within the coral tissue E_0(PAR) was fitted to an exponential decay function to estimate the diffuse attenuation coefficient of E_0(PAR), K_0(PAR) in units of mm^{-1}

$$E_0(\mathrm{PAR}, z) = E_0(\mathrm{PAR}, z_0)e^{(-K_0(\mathrm{PAR})z)}.$$

The absorption coefficient of PAR within the coral tissue was estimated from the coral tissue irradiance reflectance (R) and the scalar irradiance attenuation coefficient, K_0(PAR) as [37]

$$A(\mathrm{PAR}) = K_0 \frac{1-R}{1+R},$$

assuming that photons at each depth have equal probability to propagate in all directions, i.e. a totally diffuse light field within the tissue.

The spectral attenuation coefficient ($K_0(\lambda)$) of scalar irradiance with depth (z) was calculated as

$$K_0(\lambda) = -\frac{\ln E_0(\lambda)_1 / E_0(\lambda)_2}{z_2 - z_1},$$

where $E_0(\lambda)_1$ and $E_0(\lambda)_2$ are the spectral scalar irradiance measured at depths z_1 and z_2, respectively [40]. We used these data to identify depths within the coral tissue with the strongest light attenuation and spectral signatures of photopigments.

The local density of absorbed light $E_{ABS}(z)$ (in µmol photons m^{-3} s^{-1}) at particular depths in the coral tissue was calculated as

$$E_{ABS}(z) = \frac{A(\mathrm{PAR})}{2} E_0(z),$$

assuming a totally diffuse light field inside the tissue, i.e. photons at the given depths had equal probabilities of propagation in all directions [37].

Finally, the local photosynthetic QE, $\eta(z)$ (O_2 photon^{-1}), was calculated by dividing the locally measured volumetric GPP rates with $E_{ABS}(z)$

$$\eta(z) = \frac{\mathrm{PS}(z)}{E_{ABS}(z)}.$$

3. Results

3.1. Spectral light microenvironment

In the uppermost coral tissue layers (approx. 0–0.3 mm) there was a local enhancement in scalar irradiance relative to the incident irradiance with maximum values at the coral surface reaching 135 and 191% of the incident downwelling irradiance at 640 and 1280 µmol photons m^{-2} s^{-1}, respectively (figure 2*a*,*b*). Scalar irradiance attenuation spectra showed that the highest light attenuation occurred at the tissue–skeleton interface, especially around the absorption maxima of the predominant photopigments Chl *a* (440 and 675 nm), Chl *c* (635 nm) and the dinoflagellate carotenoid peridinin (490 nm) (figure 2*c*,*d*).

Below 0.1 mm depth, E_0(PAR) was attenuated exponentially with depth in the coral tissue (figure 3) with attenuation coefficients of 0.79 and 1.18 mm^{-1} at an incident irradiance of 640 and 1280 µmol photons m^{-2} s^{-1}, respectively. This corresponds to a decrease from 135 to 90% and 191 to 91% of the incident irradiance over a tissue thickness of 0.4 and 0.5 mm, respectively. The absorption coefficient A(PAR) in the coral tissue was calculated to be 0.628 and 0.949 mm^{-1} under a downwelling irradiance of 640 and 1280 µmol photons m^{-2} s^{-1}, respectively.

The coral tissue irradiance reflectance, R(PAR), was approximately 12 and 11% at 640 and 1280 µmol photons m^{-2} s^{-1}, respectively. Reflectance levels were constant over an irradiance range 160–2400 µmol photons m^{-2} s^{-1} and no significant correlation between reflection and incident irradiance was found ($p > 0.05$, electronic supplementary material, figure S1).

3.2. Temperature microenvironment

A slight surface heating of the coral tissue relative to the ambient seawater was observed, which increased with irradiance. A TBL could only be identified at irradiance levels more than 320 µmol photons m^{-2} s^{-1} (figure 4*a*), reaching a thickness of approximately 3 mm at a flow velocity of 0.4 cm s^{-1}. There was a positive linear correlation between the coral surface warming, ΔT, and the incident irradiance with a heating slope of 0.0023°C (J m^{-2} s^{-1})$^{-1}$, and increasing temperature gradients of 0.24–0.98°C between coral tissue and the ambient water under increasing irradiance ($R^2 = 0.98$; figure 4*b*).

3.3. O_2 microenvironment and photosynthesis

Local volumetric rates of GPP ranged between 7 and 25 nmol O_2 cm^{-3} s^{-1} and O_2 production was detected at all vertical measurement positions within the 0.5–0.7 mm thick coenosarc tissue (figure 5). Generally, GPP peaked approximately 0.1–0.3 mm below the tissue surface; however the vertical distribution of photosynthesis differed under the different experimental irradiance regimes. The O_2 microenvironment within the tissue ranged between 500 and 900 µM (240–430% air saturation) and showed in most cases an increasing trend towards the tissue–skeleton interface (figure 5).

3.4. Energy budget

Based on detailed measurements of light, photosynthesis and temperature, we calculated a balanced light energy budget in % of the incident light energy for incident downwelling photon irradiances of 640 and 1280 µmol photons m^{-2} s^{-1} (equivalent to a vector irradiance of 116 and 234 J m^{-2} s^{-1}, respectively) (figure 6). About 3.5 and 2.2% of the incident irradiance was conserved by photosynthesis, while 84.9 and 86.9% was dissipated as heat under an incident photon irradiance of 640 and 1280 µmol photons m^{-2} s^{-1}, respectively

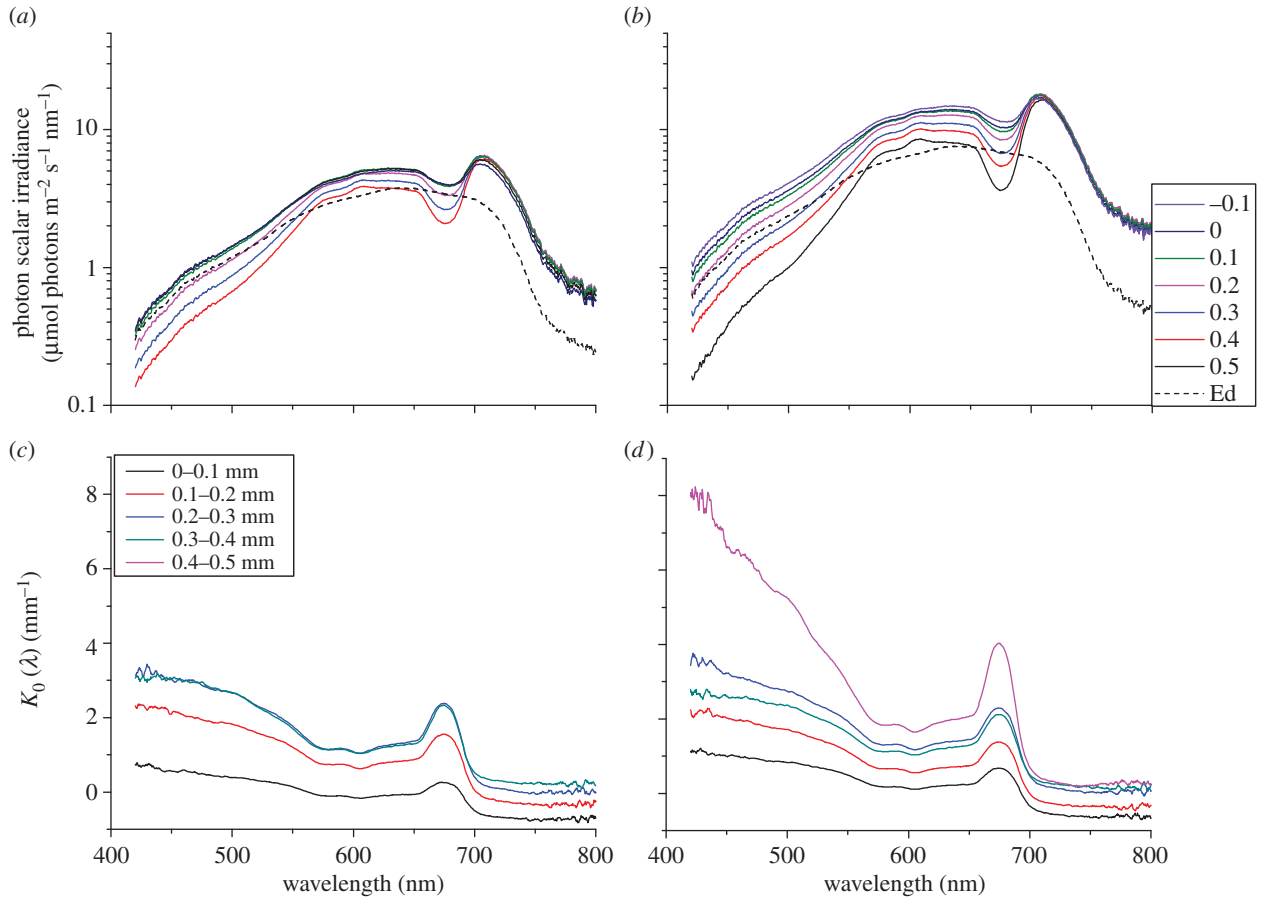

Figure 2. Photon scalar irradiance and spectral attenuation in coral tissue. Photon scalar irradiance spectra measured at two different downwelling photon irradiances of (*a*) 640 and (*b*) 1280 µmol photons m^{-2} s^{-1}. The dashed line is the incident downwelling spectral irradiance. Spectral attenuation coefficient of scalar irradiance $K_0(\lambda)$ (mm^{-1}) measured at two different downwelling photon irradiances of (*c*) 640 and (*d*) 1280 µmol photons m^{-2} s^{-1}. Legends show the measurement depth below the tissue surface (0 mm = coral tissue surface). (Spectra represent mean values; $n = 3$.)

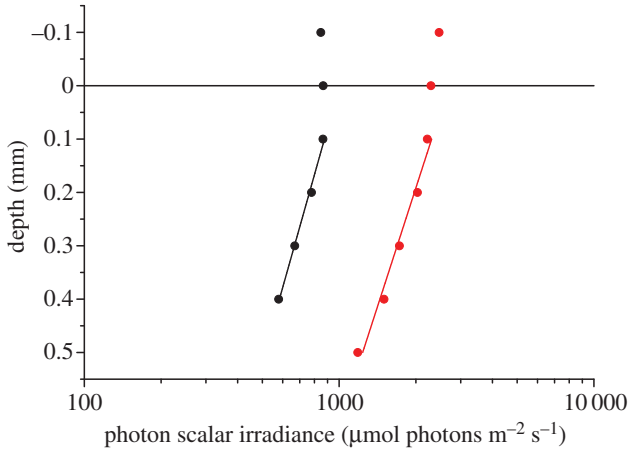

Figure 3. Vertical distribution of photon scalar irradiance (400–700 nm), E_0(PAR), in coral tissue under an incident downwelling irradiance of 640 µmol photons m^{-2} s^{-1} (black symbols) and 1280 µmol photons m^{-2} s^{-1} (red symbols) ($n = 3$, R^2 of exponential fits (solid lines) were 0.99 and 0.98, respectively). $y = 0$ indicates the position of the tissue surface.

(flow velocity of approx. 0.4 cm s^{-1}). The remaining 11.6 and 10.9% of the incident light energy was backscattered by the tissue surface and thus not absorbed.

At increased flow velocity (approx. 0.8 cm s^{-1}), the proportion of the incident light energy that was photochemically conserved decreased to 2.6 and 1.0% under an incident photon irradiance of 640 and 1280 µmol photons m^{-2} s^{-1}, respectively. Generally, the energy budget was dominated by heat dissipation and the proportion of energy conserved by photosynthesis decreased with increasing incident irradiance favouring dissipation of heat (figure 6 and table 2). The maximum efficiency of photochemical energy conservation, $\varepsilon_{PS,max}$, and the minimum efficiency of heat dissipation, $\varepsilon_{H,min}$, were 0.04 and 0.96, respectively (table 2).

Based on detailed light and photosynthesis measurements, we estimated the QE of photosynthesis in particular depths in the coral tissue (figure 7). The local QEs varied over depth, with an increasing trend towards the tissue–skeleton interface and showing decreasing QE values at increasing incident irradiances. The maximum photosynthetic QE was 0.102 O_2 $photon^{-1}$ (320 µmol photons m^{-2} s^{-1}), approaching the theoretical maximum of 0.125 O_2 $photon^{-1}$.

4. Discussion

This fine-scale study of the energy budget and photosynthetic efficiency of the symbiont-bearing scleractinian coral *M. curta* presents the first detailed account of the fate of incident and absorbed light within coral tissues. Despite the finding that a relatively high proportion of the incident irradiance (approx. 11%) was backscattered at the tissue surface and thus not absorbed (figure 6; electronic supplementary material, figure S1) we found that corals are highly efficient at using solar radiation (figure 7).

Within the coral tissue, the absorbed light differed from the incident irradiance with respect to both spectral composition

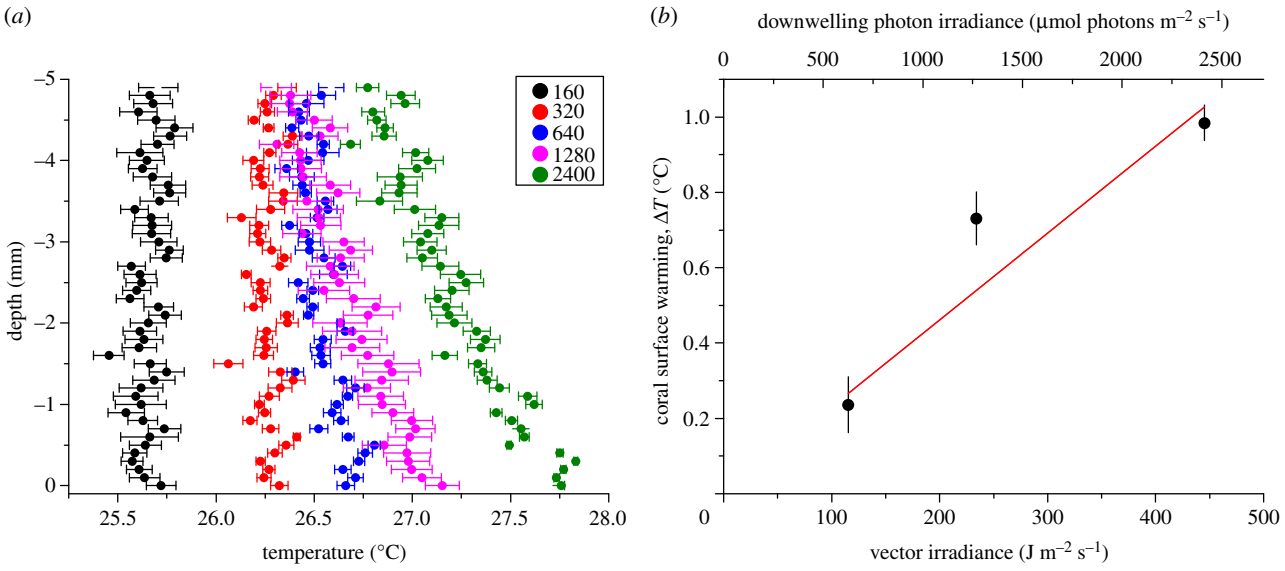

Figure 4. (*a*) Vertical microprofiles of temperature (°C) through the TBL under five different downwelling photon irradiances (160, 320, 640, 1280 and 2400 µmol photons m^{-2} s^{-1}) and a flow velocity of 0.4 cm s^{-1}. Symbols and error bars indicate mean ± s.d.; $n = 3$. (*b*) Measured temperature gradients (°C) between the ambient seawater and the coral tissue surface measured at three vector irradiances (116, 234 and 445 J m^{-2} s^{-1}). R^2 of linear fit = 0.98. Error bars are ± s.d. ($n = 3$).

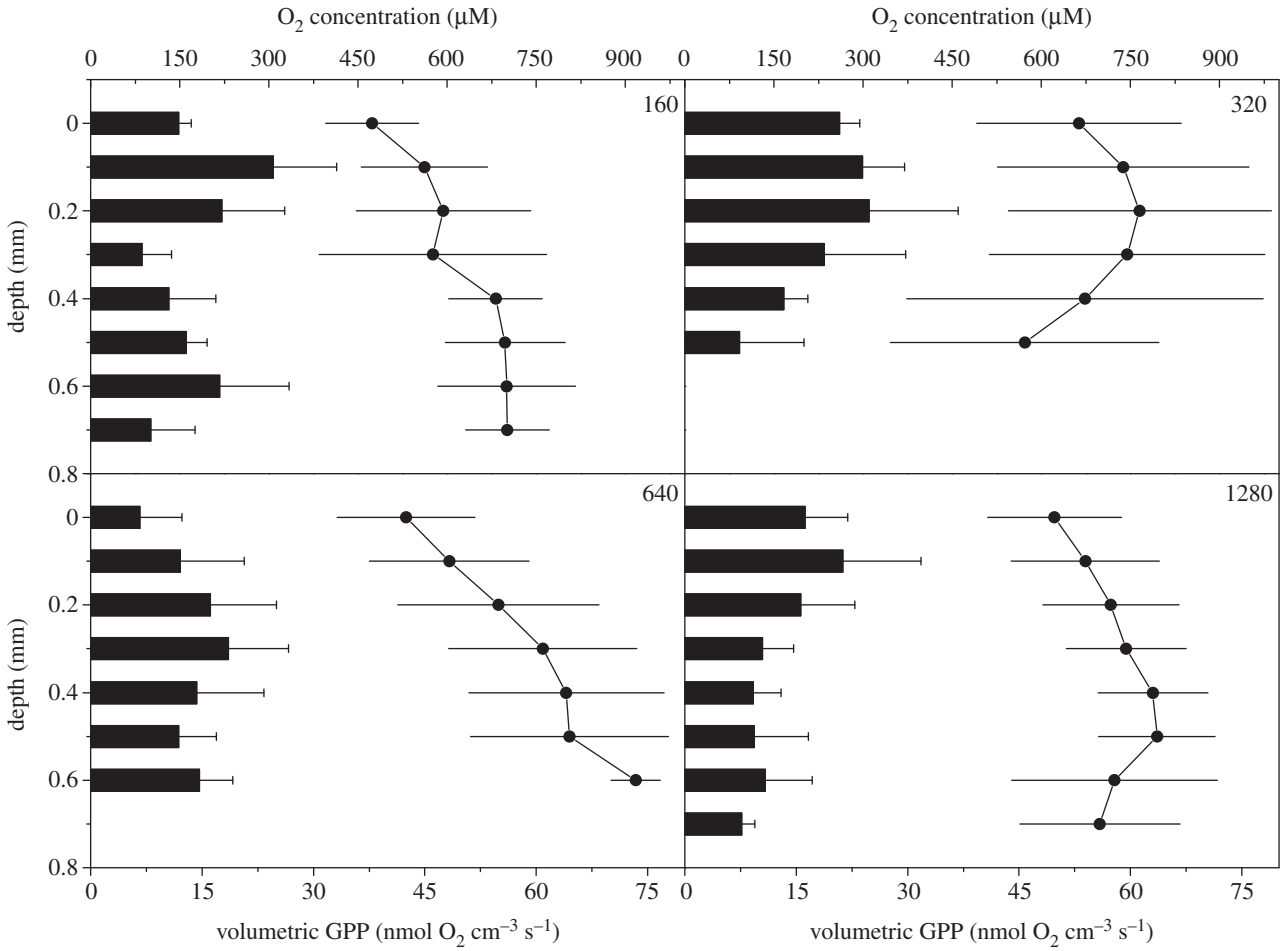

Figure 5. Vertical microprofiles of volumetric gross photosynthesis rates (in nmol O_2 cm^{-3} s^{-1}) (black bars; bottom *x*-axis) and the corresponding O_2 concentrations (in µM) (line and symbols; top *x*-axis) measured under four different downwelling photon irradiances (160, 320, 640 and 1280 µmol photons m^{-2} s^{-1}). Error bars indicate ± s.d. ($n = 3$).

and intensity, where scalar irradiance was enhanced (135 and 191% for incident irradiances of 640 µmol photons m^{-2} s^{-1} and 1280 µmol photons m^{-2} s^{-1}, respectively) at and just below the coral tissue surface (figure 2*a*,*b*). Such enhancement suggests intense scattering and redistribution of photons in the upper layers of the tissue [35]. Tissue scattering increases the local density and residence time of photons because of increased photon pathlength per vertical distance traversed [40]. These findings are similar to recent studies by Wangpraseurt *et al*. [35,36] observing scalar irradiance levels

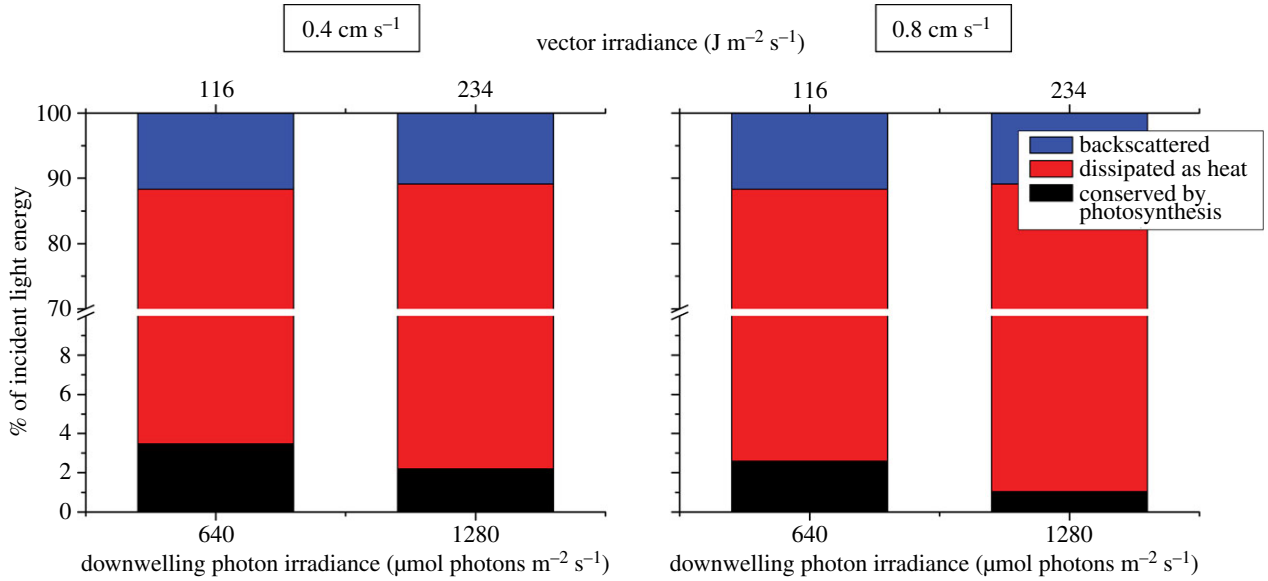

Figure 6. Light energy budget in % of the incident irradiance calculated for two downwelling photon irradiances (640 and 1280 μmol photons m^{-2} s^{-1}) and at two different flow velocities (0.4 and 0.8 cm s^{-1}). Blue bars are the fraction of energy backscattered by the coral surface, red bars are the fraction of energy dissipated as heat and black bars are fraction of energy conserved by photosynthesis. Note the break in the *y*-axis.

reaching up to 200% of the incident downwelling irradiance in the upper coral tissue layers (0–100 μm). We observed the highest attenuation of scalar irradiance in the lowest tissue depth interval, i.e. at the tissue–skeleton interface (figure 2*c*,*d*), where strong backscatter would further enhance light absorption efficiency by symbionts in the coral tissue [30].

We found a pronounced positive correlation between increasing incident irradiance and dissipation of heat, leading to the establishment of approximately 3 mm thick TBL at incident irradiances more than 320 μmol photons m^{-2} s^{-1} (figure 4*a*). We also measured a linear increase in tissue surface temperature, resulting in convective heat dissipation over a TBL, with an average slope of 2.3×10^{-3}°C (J m^{-2} s^{-1})$^{-1}$ and a maximum temperature difference of +0.98°C (figure 4*b*). Hemispherical corals studied by Jimenez *et al.* [15,18] showed a similar maximum surface warming, ΔT, between the surface tissue and the ambient water of +0.9°C, with a TBL thickness of approximately 3 mm and an average slope of approximately 1.7×10^{-3}°C (J m^{-2} s^{-1})$^{-1}$ at equivalent flow velocities and absorbed irradiances.

The rate of photosynthesis within the illuminated coenosarc coral tissue showed a relatively uniform distribution of photosynthesis throughout the tissue and O_2 concentrations ranged from 500 to 900 μM (240–430% air saturation; figure 5). This correlated with the attenuation of PAR observed within the coenosarc tissue (figures 2 and 3), where approximately 90% of the incident irradiance remained at the tissue–skeleton interface.

The coral skeleton acts as a diffusion barrier for chemical species, leading to a relative build-up of solutes (such as O_2) in the lower tissue layers (figure 5). This has recently been shown to increase the O_2 concentration up to approximately 400% of air saturation at the tissue–skeleton interface [35]. Saturation of photosynthetic activity at high irradiance led to decreased photosynthetic efficiencies, i.e. a decreased proportion of the absorbed light energy was conserved by photosynthesis with increasing incident irradiances (figure 6 and table 2). At increased flow velocity (approx. 0.8 cm s^{-1}), the proportion of the absorbed light energy conserved by photosynthesis decreased as compared to the lower flow velocity (approx. 0.4 cm s^{-1}; figure 6). This was unexpected as a decrease in boundary layer thickness owing to increased flow rates normally leads to increased rates of photosynthesis and respiration as a response to alleviation of mass transfer resistance for O_2 and dissolved inorganic carbon exchange [48,49]. However, we also saw a decreased euphotic zone (i.e. the photosynthetic tissue layer) from approximately 0.6 to 0.4 mm, possibly owing to coenosarc tissue contraction at higher flow. Recently, tissue contraction has been found to reduce the amount of lateral light transfer through coral tissue and could thus explain the observed reduction in local GPP rates [36].

The volumetric rates of photosynthesis at higher flow were of the same order as at the lower flow velocity, i.e. PS_{max} of 24.2 nmol O_2 cm^{-3} s^{-1} (data not shown). At a flow velocity of approximately 0.8 cm s^{-1}, the proportion of the absorbed light energy that was used in photosynthesis still represents a high energy efficiency (figure 6 and table 2) as compared to other photosynthetic systems such as biofilms and microbial mats, where less than 1.8% of the absorbed light energy was conserved by photosynthesis at equivalent vector irradiances [37].

In comparison with previous studies of the radiative energy budget of benthic photosynthetic systems, such as biofilms and microbial mats [37,50], we found much higher photosynthetic efficiencies in coral tissue. Locally measured volumetric rates of photosynthesis in the coral tissue were very high (up to 25 nmol O_2 cm^{-3} s^{-1}; figure 5) as compared to what has been reported in microbial mats and biofilms (Australian mat 6–13 nmol O_2 cm^{-3} s^{-1}, Abu Dhabi mat 2–6 nmol O_2 cm^{-3} s^{-1} [37,50]) at equivalent absorbed irradiances. Even when considering the relatively restricted spatial extension of photosynthesis in corals (*M. curta* approx. 0.5 mm tissue thickness) as compared to an order of photic zone of approximately 1–2 mm in microbial mats and biofilms, the depth integrated areal rate of photosynthesis, i.e. the photosynthetic energy conservation of the coral system (P_{max} = 5.8 J m^{-2} s^{-1}; table 2), was about three times higher than what has been reported in biofilms and microbial mats at equivalent absorbed irradiances.

A high light usage efficiency in corals was also supported by our measurements of the local QE of photosynthesis

Table 2. Balanced light energy budget (in energy units), overall photosynthetic energy use and heat dissipation (in % of absorbed light energy) and efficiencies of photochemical energy conservation and heat dissipation (ε_{PS} and ε_H) at two different incident irradiances and flow velocities.

	J_{PS} (J m^{-2} s^{-1})		J_H (J m^{-2} s^{-1})		ε_{PS}		ε_H		$\varepsilon_{PS} + \varepsilon_H$
J_{ABS} (J m^{-2} s^{-1})	0.4 cm s^{-1}	0.8 cm s^{-1}	0.4 cm s^{-1}	0.8 cm s^{-1}	0.4 cm s^{-1}	0.8 cm s^{-1}	0.4 cm s^{-1}	0.8 cm s^{-1}	both flow velocities
116	4.55 (3.9%)	3.39 (2.9%)	111.0 (96.1%)	112.2 (97.1%)	0.04	0.03	0.96	0.97	1.0
234	5.77 (2.5%)	2.71 (1.2%)	228.1 (97.5%)	231.2 (98.8%)	0.02	0.01	0.98	0.99	1.0

Figure 7. Vertical microprofiles of the local photosynthetic quantum efficiency (QE) (η) in the studied coral (in units of mol O_2 produced per mol photon absorbed) under three different incident photon irradiances noted as colour bar legends (in μmol photons m^{-2} s^{-1}). $y = 0$ indicates the position of the tissue surface.

showing much higher values than in biofilms or other compact photosynthetic systems of similar thickness and degree of compaction [50]. The local QE generally decreased with increasing incident downwelling irradiances but the maximum QE of 0.102 O_2 per photon under a photon irradiance of 320 μmol photons m^{-2} s^{-1} (figure 7) approached the theoretical maximum of 0.125. Such high efficiency values are about an order of magnitude higher than previous estimates that were based on tissue extracts and thus ignored the role of coral tissue and skeleton optics in light absorption efficiency [51–54]. More similar but still lower QEs were reported when coral absorptance was based on skeleton reflectivity (approx. 0.07 mol O_2 per absorbed mol photons [32]). Likewise, a study of intact colonies of the coral *Montipora monasteriata* in shaded environments also showed high QE values of 0.071–0.096 O_2 per incident photon [55]. Such high efficiencies are comparable to macroalgal stands and terrestrial communities such as forests, which exhibit a canopy distribution of the photosynthetic active components facilitating a more uniform availability and use of light throughout the photic zone [56,57]. It is thus intriguing to speculate whether microscale canopy effects are at play in corals that facilitate the observed high photosynthetic efficiency.

Light regulation on a microscale occurs through several mechanisms in corals. Photons incident on the coral surface will be strongly scattered in the coral tissue. This enhances photon pathlength per vertical distance traversed and thus the average residence time of photons at a given point within the tissue increasing the probability of absorption for wavelengths overlapping with absorption maxima of symbiont photopigments or coral host pigments [35]. In combination with refractive index mismatches between coral tissue and water such photon trapping leads to near-surface maxima in scalar irradiance and enhanced spectral filtering [40]. Light can also be transferred laterally through coral tissue thereby leading to a more homogeneous distribution of incident irradiance over the coral [36]. Additionally, photons that have passed through tissue undergo multiple scattering in the coral skeleton, which acts as a Lambertian-like diffuser and thus facilitates further enhancement of

light capture by zooxanthellae [30,58]. Corals thus have several distinct microscale mechanisms that can optimize light capture and usage.

Light regulating mechanisms also operate on larger scales. It is known that individual colonies show a plastic response to the ambient light climate, where for instance coral orientation, branch spacing and corallite architecture are regulated by the ambient light climate [59–63]. The concerted action of the mentioned micro- and macroscale light regulating mechanisms indeed indicates that symbiont-bearing corals have canopy-like optical properties not only at larger colony and reef scales but also at the scale of single polyps, where optical properties of tissue and skeleton act in with behavioural modulation of tissue contraction/expansion [36,64] to maintain high QEs and metabolic rates.

In conclusion, we present the first balanced radiative energy budget of a symbiont-bearing coral. The majority (more than 96%) of absorbed light energy was dissipated as heat and the proportion of the absorbed light energy that was photochemically conserved decreased with increasing incident irradiance favouring heat dissipation. Yet, coral symbionts are able to retain a very high photosynthetic activity and efficiency *in hospite*, and we propose that canopy-like effects involving the interplay between tissue and skeleton optical properties of the coral holobiont are important but largely unexplored factors affecting the successful algal–cnidarian symbiosis and its ability to adapt to different light regimes.

Acknowledgements. We thank the staff at Heron Island Research Station for excellent assistance during our field work and Dr V. Schrameyer and Dr D. Nielsen for thoughtful discussions. We acknowledge the help and assistance from the Aquatic Processes Group at the University of Technology, Sydney (UTS). The research was conducted under research permits for field work on the Great Barrier Reef, Australia (G11/34670.1 and G09/31733.1) and was funded by grants from Knud Højgaards Fond, Oticon Fonden, Thorsons Rejselegat, København Universitets Fælleslegat (Pastor Peter Albert Raashous legat) (K.E.B. and M.L.), the Danish Council for Independent Research | Natural Sciences (M.K.), the Australian Research Council (P.J.R. and M.K.) and the University of Technology, Sydney (K.E.B. and D.W.). K.E.B., M.L., D.W. and M.K. designed research and outlined experiments. K.E.B., M.L. and D.W. conducted experiments. K.E.B., M.L., D.W. and M.K. analysed data. P.J.R. and M.K. contributed new analytical tools. K.E.B., D.W. and M.K. wrote the paper with editorial inputs from M.L. and P.J.R.

References

1. Muscatine L, McCloskey L, Marian R. 1981 Estimating the daily contribution of carbon from zooxanthellae to coral animal respiration. *Limnol. Oceanogr.* **26**, 601–611. (doi:10.4319/lo.1981.26.4.0601)
2. Edmunds PJ, Spencer Davies P. 1986 An energy budget for *Porites porites* (Scleractinia). *Mar. Biol.* **92**, 339–347. (doi:10.1007/BF00392674)
3. Falkowski P, Raven J. 1997 *Aquatic photosynthesis*. Oxford, UK: Blackwell Science.
4. Kirk J. 2007 *Light and photosynthesis in aquatic ecosystems*, 3rd ed. Cambridge, UK: Cambridge University Press.
5. Müller P, Li X, Niyogi K. 2001 Non-photochemical quenching. A response to excess light energy. *Plant Physiol.* **125**, 1558–1566. (doi:10.1104/pp.125.4.1558)
6. Nymark M, Valle K, Brembu T, Hancke K, Winge P, Andresen K, Johnsen G. 2009 An integrated analysis of molecular acclimation to high light in the marine diatom *Phaeodactylum tricornutum*. *PLoS ONE* **4**, e7743. (doi:10.1371/journal.pone.0007743.t001)
7. Bartley GE, Scolnik PA. 1995 Plant carotenoids: pigments for photoprotection, visual attraction, and human health. *Plant Cell* **7**, 1027–1038. (doi:10.1105/tpc.7.7.1027)
8. Falkowski PG, Dubinsky Z. 1981 Light-shade adaptation of *Stylophora pistillata*, a hermatypic coral from the Gulf of Eilat. *Nature* **289**, 172–174. (doi:10.1038/289172a0)
9. Salih A, Larkum A, Cox G, Kühl M, Hoegh-Guldberg O. 2000 Fluorescent pigments in corals are photoprotective. *Nature* **408**, 850–853. (doi:10.1038/35048564)
10. D'Angelo C, Denzel A, Vogt A, Matz MV, Oswald F, Salih A, Nienhaus GU, Wiedenmann J. 2008 Blue light regulation of host pigment in reef-building corals. *Mar. Ecol. Progr. Ser.* **364**, 97–106. (doi:10.3354/meps07588)
11. Dove SG, Lovell C, Fine M, Deckenback J, Hoegh-Guldberg O, Iglesias-Prieto R, Anthony KRN. 2008 Host pigments: potential facilitators of photosynthesis in coral symbioses. *Plant Cell Environ.* **31**, 1523–1533. (doi:10.1111/j.1365-3040.2008.01852.x)
12. Smith E, D'Angelo C, Salih A, Wiedenmann J. 2013 Screening by coral green fluorescent protein (GFP)-like chromoproteins supports a role in photoprotection of zooxanthellae. *Coral Reefs* **32**, 463–474. (doi:10.1007/s00338-012-0994-9)
13. Schlichter D, Fricke HW. 1990 Coral host improves photosynthesis of endosymbiotic algae. *Naturwissenschaften* **77**, 447–450. (doi:10.1007/BF01135950)
14. Alieva NO *et al*. 2008 Diversity and evolution of coral fluorescent proteins. *PLoS ONE* **3**, e2680. (doi:10.1371/journal.pone.0002680)
15. Jimenez IM, Kühl M, Larkum AWD. 2008 Heat budget and thermal microenvironment of shallow-water corals: do massive corals get warmer than branching corals? *Limnol. Oceanogr.* **53**, 1548–1561. (doi:10.4319/lo.2008.53.4.1548)
16. Jimenez IM, Larkum AWD, Ralph PJ, Kühl M. 2012 *In situ* thermal dynamics of shallow water corals is affected by tidal patterns and irradiance. *Mar. Biol.* **8**, 1773–1782. (doi:10.1007/s00227-012-1968-8)
17. Jimenez IM, Larkum AWD, Ralph PJ, Kühl M. 2012 Thermal effects of tissue optics in symbiont-bearing reef building corals. *Limnol. Oceanogr.* **57**, 1816–1825. (doi:10.4319/lo.2012.57.6.1816)
18. Jimenez IM, Kühl M, Larkum AWD, Ralph PJ. 2011 Effects of flow and colony morphology on the thermal boundary layer of corals. *J. R. Soc. Interface* **8**, 1785–1795. (doi:10.1098/rsif.2011.0144)
19. Atkinson M, Bilger R. 1992 Effects of water velocity on phosphate uptake in coral reef-flat communities. *Limnol. Oceanogr.* **37**, 273–279. (doi:10.4319/lo.1992.37.2.0273)
20. Kühl M, Cohen Y, Dalsgaard T, Jørgensen BB, Revsbech NP. 1995 The microenvironment and photosynthesis of zooxanthellae in scleractinian corals studied with microsensors for O_2, pH and light. *Mar. Ecol. Progr. Ser.* **117**, 159–172. (doi:10.3354/meps117159)
21. Wangpraseurt D, Weber M, Roy H, Polerecky L, de Beer D, Suharsono, Nugues MM. 2012 *In situ* oxygen dynamics in coral–algal interactions. *PLoS ONE* **7**, e31192. (doi:10.1371/journal.pone.0031192)
22. Edmunds PJ. 2005 Effect of elevated temperature on aerobic respiration of coral recruits. *Mar. Biol.* **146**, 655–663. (doi:10.1007/s00227-004-1485-5)
23. Finelli C, Helmuth B, Pentcheff N, Wethey D. 2006 Water flow influences oxygen transport and photosynthetic efficiency in corals. *Coral Reefs* **25**, 47–57. (doi:10.1007/s00338-005-0055-8)
24. Veal C, Carmi M, Dishon G, Sharon Y, Michael K, Tchernov D, Hoegh-Guldberg O, Fine M. 2010 Shallow-water wave lensing in coral reefs: a physical and biological case study. *J. Exp. Biol.* **213**, 4303–4312. (doi:10.1242/jeb.044941)
25. Lesser M. 1996 Elevated temperatures and ultraviolet radiation cause oxidative stress and inhibit photosynthesis in symbiotic dinoflagellates. *Limnol. Oceanogr.* **41**, 271–283. (doi:10.4319/lo.1996.41.2.0271)
26. Jones R, Hoegh-Guldberg O, Larkum AWD, Schreiber U. 1998 Temperature-induced bleaching of corals begins with impairment of the CO_2 fixation mechanism in

zooxanthellae. *Plant Cell Environ.* **21**, 1219–1230. (doi:10.1046/j.1365-3040.1998.00345.x)

27. Warner M, Fitt W, Schmidt G. 1999 Damage to photosystem II in symbiotic dinoflagellates: a determinant of coral bleaching. *Proc. Natl Acad. Sci. USA* **96**, 8007–8012. (doi:10.1073/pnas.96.14.8007)
28. Weis VM. 2008 Cellular mechanisms of Cnidarian bleaching: stress causes the collapse of symbiosis. *J. Exp. Biol.* **211**, 3059–3066. (doi:10.1242/jeb.009597)
29. Wiedenmann J, D'Angelo C, Smith EG, Hunt AN, Legiret FE, Postle AD, Achterberg EP. 2013 Nutrient enrichment can increase the susceptibility of reef corals to bleaching. *Nat. Clim. Change* **3**, 160–164. (doi:10.1038/nclimate1661)
30. Enriquez S, Mendez ER, Iglesias-Prieto R. 2005 Multiple scattering on coral skeletons enhances light absorption by symbiotic algae. *Limnol. Oceanogr.* **50**, 1025–1032. (doi:10.4319/lo.2005.50.4.1025)
31. Stambler N, Dubinsky Z. 2005 Corals as light collectors: an integrating sphere approach. *Coral Reefs* **24**, 1–9. (doi:10.1007/s00338-004-0452-4)
32. Rodriquez-Roman A, Hernandez-Pech X, Thome PE, Enriquez S, Iglesias-Prieto R. 2006 Photosynthesis and light utilization in the Caribbean coral *Montastraea faveolata* recovering from a bleaching event. *Limnol. Oceanogr.* **51**, 2702–2710. (doi:10.4319/lo.2006.51.6.2702)
33. Pinchasov-Grinblat Y, Mauzerall D, Goffredo S, Falini G, Dubinsky Z. 2013 Photoacoustics: a novel application to the determination of photosynthetic efficiency in zooxanthellate hermatypes. *Limnol. Oceanogr. Meth.* **11**, 374–381. (doi:10.4319/lom.2013.11.374)
34. Hochberg E, Atkinson M. 2008 Coral reef benthic productivity based on optical absorptance and light-use efficiency. *Coral Reefs* **27**, 49–59. (doi:10.1007/s00338-007-0289-8)
35. Wangpraseurt D, Larkum A, Ralph P, Kühl M. 2012 Light gradients and optical microniches in coral tissues. *Front. Microbiol.* **3**, 316. (doi:10.3389/fmicb.2012.00316)
36. Wangpraseurt D, Larkum AWD, Franklin J, Szabo M, Ralph PJ, Kühl M. In press. Lateral light transfer ensures efficient resource distribution in symbiont-bearing corals. *J. Exp. Biol.*
37. Al-Najjar M, de Beer D, Jørgensen BB, Kühl M, Polerecky L. 2010 Conversion and conservation of light energy in a photosynthetic microbial mat ecosystem. *ISME J.* **4**, 440–449. (doi:10.1038/ismej.2009.121)
38. Lassen C, Ploug H, Jørgensen BB. 1992 A fibre optic scalar irradiance microsensor—application for spectral light measurements in sediments. *FEMS Microbiol. Ecol.* **86**, 247–254. (doi:10.1111/j.1574-6968.1992.tb04816.x)
39. Lassen C, Ploug H, Jørgensen BB. 1992 Microalgal photosynthesis and spectral scalar irradiance in coastal marine sediments of Limfjorden, Denmark. *Limnol. Oceanogr.* **37**, 760–772. (doi:10.4319/lo.1992.37.4.0760)
40. Kühl M, Jørgensen BB. 1994 The light field of microbenthic communities: radiance distribution and microscale optics of sandy coastal sediments. *Limnol. Oceanogr.* **39**, 1368–1398. (doi:10.4319/lo.1994.39.6.1368)
41. Jørgensen BB, Marais D. 1988 Optical properties of benthic photosynthetic communities: fiber-optic studies of cyanobacterial mats. *Limnol. Oceanogr.* **33**, 99–113. (doi:10.4319/lo.1988.33.1.0099)
42. Kühl M. 2005 Optical microsensors for analysis of microbial communities. *Meth. Enzymol.* **397**, 166–199. (doi:10.1016/S0076–6879(05)97010–9)
43. Revsbech NP. 1989 An oxygen microsensor with a guard cathode. *Limnol. Oceanogr.* **34**, 474–478. (doi:10.4319/lo.1989.34.2.0474)
44. Revsbech NP. 1989 Diffusion characteristics of microbial communities determined by use of oxygen microsensors. *J. Microbiol. Meth.* **9**, 111–122. (doi:10.1016/0167-7012(89)90061-4)
45. Revsbech NP, Jørgensen BB. 1983 Photosynthesis of benthic microflora measured with high spatial resolution by the oxygen microprofile method: capabilities and limitations of the method. *Limnol. Oceanogr.* **28**, 749–756. (doi:10.4319/lo.1983.28.4.0749)
46. Thauer R, Jungermann K, Decker K. 1977 Energy conservation in chemotrophic anaerobic bacteria. *Bacteriol. Rev.* **41**, 100–180.
47. Young H, Freedman R, Ford L. 1996 *University physics, with modern physics*. Boston, MA: Addison Wesley.
48. Kühl M, Glud RN, Ploug H, Ramsing NB. 1996 Microenvironmental control of photosynthesis and photosynthesis-coupled respiration in an epilithic cyanobacterial biofilm. *J. Phycol.* **32**, 799–812. (doi:10.1111/j.0022-3646.1996.00799.x)
49. Larkum AWD, Koch EM, Kühl M. 2003 Diffusive boundary layers and photosynthesis of the epilithic algal community of coral reefs. *Mar. Biol.* **142**, 1073–1082. (doi:10.1007/s00227-003-1022-y)
50. Al-Najjar M, de Beer D, Kühl M, Polerecky L. 2012 Light utilization efficiency in photosynthetic microbial mats. *Environ. Microbiol.* **14**, 982–992. (doi:10.1111/j.1462-2920.2011.02676.x)
51. Dubinsky Z, Falkowski P, Porter J, Muscatine L. 1984 Absorption and utilization of radiant energy by light- and shade-adapted colonies of the hermatypic coral *Stylophora pistillata*. *Proc. R. Soc. Lond. B* **222**, 203–214. (doi:10.1098/rspb.1984.0059)
52. Wyman KD, Dubinsky Z, Porter JW, Falkowski PG. 1987 Light absorption and utilization among hermatypic corals: a study in Jamaica, West Indies. *Mar. Biol.* **96**, 283–292. (doi:10.1007/BF00427028)
53. Dubinsky Z, Stambler N, Ben-Zion M, Mccloskey LR, Muscatine L, Falkowski P. 1990 The effect of external nutrient resources on the optical properties and photosynthetic efficiency of *Stylophora pistillata*. *Proc. R. Soc. Lond. B* **239**, 231–246. (doi:10.1098/rspb.1990.0015)
54. Lesser MP, Mazel C, Phinney D, Yentsch CS. 2000 Light absorption and utilization by colonies of the congeneric hermatypic corals *Montastraea faveolata* and *Montastraea cavernosa*. *Limnol. Oceanogr.* **45**, 76–86. (doi:10.4319/lo.2000.45.1.0076)
55. Anthony KRN, Hoegh-Guldberg O. 2003 Variation in coral photosynthesis, respiration and growth characteristics in contrasting light microhabitats: an analogue to plants in forest gaps and understoreys? *Funct. Ecol.* **17**, 246–259. (doi:10.1046/j.1365-2435.2003.00731.x)
56. Sand-Jensen K, Krause-Jensen D. 1997 Broad-scale comparison of photosynthesis in terrestrial and aquatic plant communities. *Oikos* **80**, 203–208. (doi:10.2307/3546536)
57. Krause-Jensen D, Sand-Jensen K. 1998 Light attenuation and photosynthesis of aquatic plant communities. *Limnol. Oceanogr.* **43**, 396–407. (doi:10.4319/lo.1998.43.3.0396)
58. Marcelino LA *et al*. 2013 Modulation of light-enhancement to symbiotic algae by light-scattering in corals and evolutionary trends in bleaching. *PLoS ONE* **8**, e61492. (doi:10.1371/journal.pone.0061492)
59. Helmuth BST, Timmerman BEH, Sebens KP. 1997 Interplay of host morphology and symbiont microhabitat in coral aggregations. *Mar. Biol.* **130**, 1–10. (doi:10.1007/s002270050219)
60. Anthony KRN, Hoogenboom MO, Connolly SR. 2005 Adaptive variation in coral geometry and the optimization of internal colony light climates. *Funct. Ecol.* **19**, 17–26. (doi:10.1111/j.0269-8463.2005.00925.x)
61. Hoogenboom MO, Connolly SR, Anthony KRN. 2008 Interactions between morphological and physiological plasticity optimize energy acquisition in corals. *Ecology* **89**, 1144–1154. (doi:10.1890/07-1272.1)
62. Ow Y, Todd P. 2010 Light-induced morphological plasticity in the scleractinian coral *Goniastrea pectinata* and its functional significance. *Coral Reefs* **29**, 797–808. (doi:10.1007/s00338-010-0631-4)
63. Kaniewska P, Anthony KRN, Sampayo EM, Campbell PR, Hoegh-Guldberg O. In press. Implications of geometric plasticity for maximizing photosynthesis in branching corals. *Mar. Biol.* (doi:10.1007/s00227-013-2336-z)
64. Levy O, Dubinsky Z, Achituv Y. 2003 Photobehavior of stony corals: responses to light spectra and intensity. *J. Exp. Biol.* **206**, 4041–4049. (doi:10.1242/jeb.00622)